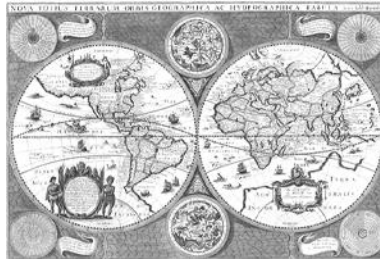


Spruce Beetle (*Dendroctonus rufipennis*) Infestation for the Cook Inlet Ecoregion, Alaska

By

Michael Tuffly, Ph.D.

ERIA Consultants, LLC



Email: mtuffly@eriaconsultants.com

URL: <http://www.eriaconsultants.com>

Phone: 303 449 5146

165 South 32nd Street

Boulder, CO 80305, USA

7/3/2019

Contents

Introduction.....	3
Methods.....	4
Results.....	6
Accuracy Assessment	8
Discussion	8
References	31
Figure 1	12
Figure 2	13
Figure 3	14
Figure 4	15
Figure 5	16
Figure 6	17
Figure 7	18
Figure 8	19
Figure 9. Classification and Regression Tree output for 2017.	19
Figure 10. Classification and Regression Tree output for 2018.	20
Figure 11	21
Figure 12	22
Figure 13	23
Figure 14	24
Figure 15	25
Figure 16	26
Figure 17. Data Processing Flow Chart.	27
Table 1. Elevation Ranges.	28
Table 2. Basal Area Ranges.	28
Table 3. Probability of spruce mortality due to <i>D. rufipennis</i> in the Cook Inlet 2017.	28
Table 4. Probability of spruce mortality due to <i>D. rufipennis</i> in the Cook Inlet 2018.	28
Table 5. Potential spruce basal area loss per acre in the Cook Inlet due to <i>D. rufipennis</i> 2017.	29
Table 6. Potential spruce basal area loss per acre in the Cook Inlet due to <i>D. rufipennis</i> 2018.	29
Table 7. Probability of spruce mortality due to <i>D. rufipennis</i> in the Cook Inlet 2019.	29
Table 8. Potential spruce basal area loss per acre in the Cook Inlet due to <i>D. rufipennis</i> 2019.	29
Table 9. Confusion Matrix 2017.	30
Table 10. Confusion Matrix 2018.	30

Introduction

The study area for this project is the Cook Inlet ecoregion in Alaska (EPA 2013) (figure 1). The Cook Inlet ecoregion is 3,038,642 hectares in size. The 3,038,642 hectares encompassing the Cook Inlet holds 53,988 hectares of water in the form of lakes. The Cook Inlet contains elevations that range from a low of -6 meters to a high of 1936 meters (figure 2) (table 1).

Spruce trees (*Picea* spp.) are the dominate terrestrial conifer vegetation covering the landscape of the Cook Inlet. The ecoregion contains spruce trees that range from 0 to 250 (USFS 2019) square feet of basal area per acre. The spatial distribution of basal area per acre of *Picea* is contained in figure 3 and the percent area by basal area classes are contained in table 2.

Spruce beetle (*Dendroctonus rufipennis* Kirby) is a widely distributed North American endemic bark beetle (Coleoptera: Curculionidae: Scolytinae) (Sherriff, Berg et al. 2011). *D. rufipennis* host species are spruce trees (*Picea* spp.). That is, *D. rufipennis* attacks and kills spruce trees from Arizona to Alaska. The life cycle of *D. rufipennis* is labeled as bivoltine (one generation every two-years) (Fairweather, McMillin et al. 2006). In addition, *D. rufipennis* is also known to carry the infection vector for the blue stain fungus. The blue stain fungus (genera *Ophiostoma* and *Ceratocystis*) is also a primary mortality agent affecting spruce trees (Hagle, Gibson et al. 2003).

After a spruce tree is attacked by *D. rufipennis* tree mortality usually occurs two or more years after initial infestation. Therefore, when detecting infestations of *D. rufipennis* from aerial surveys a lag time is likely to occur. This lag time is compounded by both the time that occurs for the spruce trees to die, thus being ocularly detected from an airplane, and the bivoltine life cycle of *D. rufipennis*.

D. rufipennis outbreaks often occur in spruce stands that are growing on poor soils, over mature, weakened or stressed by other causal agent such as diseases (i.e. root rot) or physically damaged by wildfire, drought, flooding, wind-throw or avalanches (van Driesche, Laforest et al. 2019). Tuffly (2012) concluded that when plant defenses are compromised and populations of deleterious insects are present in sufficient numbers; then, the likelihood of infestation is exacerbated.

It has been estimated that global average air temperatures are rising by 1° C to 5° C (Williams and Liebhold 2002). Forrest (2016) states that warmer temperatures can speed up insect development and thus change voltinism from two-years to one. Moreover, Sherriff, Berg and Miller (2011) suggest that warmer air temperatures greatly facilitates *D. rufipennis* outbreaks in south central Alaska. Finally, Williams and Liebhold (2002) have documented that two North American endemic bark beetles (*Dendroctonus frontalis* and *Dendroctonus ponderosae*) populations have shifted to higher elevations and higher latitudes due to warmer air temperatures. This may be an indication that in the next few decades *D. rufipennis* populations in Alaska will surge; subsequently, increasing the mortality of spruce trees over the landscape.

Over the past 25-years optical multispectral data from both the LandSat project and the Moderate Resolution Imaging Spectroradiometer (MODIS) project (NASA 2019) have been a mainstay in assessing and quantifying the status of vegetation over large landscapes. Optical multispectral data is plague by any phenomena that alters optical reflectance. Some of the main reflectance altering phenomena are: clouds, atmospheric aerosols, and sun angles.

In the Cook Inlet ecoregion, clouds and varying sun angles are the biggest deterrent to optical multispectral data. The Google Earth Engine (GEE) Application Programming Interface (API) has partly resolved the cloud issue with optical multispectral data. That is, using the computing power of Google's® massive computers coupled with the GEE API users can write computer programs that can search the Landsat and MODIS data archive, for an area of interest, and over a particular time period, for optical multispectral data that is relatively cloud free. This can produce imagery that is relatively cloud free but from different time periods. Finally, the GEE API can concatenate the cloud free imagery from varying time periods into a single comprehensive scene for the area of interest.

However, obtaining cloud free imagery from different time periods exacerbates the sun angle issue. Sun angles produce shadows over the landscape. Shadows mask the true optical reflectance properties of the object of interest. Furthermore, in the northern latitudes, of the Cook Inlet, sun angles differ greatly from season to season. Consequently, classifying optical images from different time periods in the Cook Inlet may intensify image anomalies due to varying sun angles over the study area.

Synthetic Aperture Radar (SAR) relies on microwaves to collect information. Microwaves are not influenced by clouds, atmospheric aerosols, or sun angles (SERVIR 2019). The Sentinel-1 Copernicus (ESA 2018) satellite collects data in the C-band. The C-band has wavelengths that are from four to eight centimeters in size (Moreira, Prats-Iraola et al. 2013).

The long wave length of the SAR C-band is relative to the size of forest canopy elements (i.e. leaves, branches, and stems) (Fernandez-Ordonez, Soria-Ruiz et al. 2009). Optical multispectral remotely sensed data has a much smaller wavelength (i.e. 0.4 to 2.5 micrometers). The small wave length of the optical remotely sensed data is sensitive to plant pigments (Fernandez-Ordonez, Soria-Ruiz and Leblon 2009). Concluding, that SAR data is better at identifying forest structure; whereas, optical remotely sensed data is a better tool for identifying forest condition (Fernandez-Ordonez, Soria-Ruiz and Leblon 2009).

A two-year time period spatial analysis was conducted for the Cook Inlet ecoregion of Alaska (EPA 2013) (figure 1). The purpose of this study was two-fold. First, to assess and evaluate the potential spatial and temporal extent of spruce mortality due to *D. rufipennis* infestation in the Cook Inlet ecoregion. Second, was to assess the potential spruce basal area loss due to *D. rufipennis*. The time periods assessed for this study were 2017 and 2018. A third time period, 2019, was forecasted using data from the two aforementioned time periods.

Methods

Two Aerial Detection Surveys (ADS) spatial data sets were provided by USFS (2019). One data set was for 2017 and the other was for 2018. These ADS data identified forest mortality coupled with the causal agents for selected areas in the Cook Inlet ecoregion on an annual basis.

Forest mortality polygons resulting from *D. rufipennis* were identified and isolated from the ADS data by year. In addition, polygons that were surveyed; but, contained no forest mortality were also identified and isolated. In order for a polygon to be identified as positive with *D. rufipennis* the ADS data had to reflect a minimum percent mortality of 30% and identify the causal agent as *D. rufipennis*. This ADS mortality selection process isolated two mortality groups. That is, one group was identified with a

minimum mortality of 30% and a second with a minimum mortality of 50%. Next, these two mortality groups were pooled and assigned a single mid-range value of 40% mortality (i.e. the midpoint between 30% and 50% is 40%). Finally, the positive and negative infested polygons were merged into a single comprehensive data set for the ecoregion. This resulted in a binary data set where positive polygons illustrated 40% forest mortality due to *D. rufipennis* and negative polygons illustrated 0% forest mortality due to *D. rufipennis*. The ADS positive and negative data area contained in figure 4 for 2017 and figure 5 for 2018.

A spruce basal area data set from the USFS (2019) was used as a primary filter for the ADS polygons. That is, spruce is the host species for *D. rufipennis*. So, where spruce trees are not growing there should be no possibility of infestation. Therefore, both positive and negative ADS polygons needed to contain at least one square foot of spruce basal area per acre to be included in the model.

Using ESRI (2019) geographic information system (GIS) ArcGIS® software random sample points were assigned by year to the positive and negative ADS polygons. That is, in 2017 3,500 points were assigned to the negative polygons and 2,000 points were assigned to the positive (total sample points were equal to 5,500) (figure 6). In 2018 6,323 points were assigned to the negative areas; whereas, 2,000 points were assigned to the positive areas (total equals 8,323 sample points) (figure 7).

Ancillary data was then collected and assimilated. Ancillary data consisted of two sets of optical remotely sensed data for each year. One set of optical remotely sensed data, was the Moderate Resolution Imaging Spectroradiometer (MODIS) (NASA 2019). The MODIS data had a ground sample distance (GSD) of 240-meters. The other optical data was LandSat-8 Operational Land Instrument (OLI) (NASA 2013). The LandSat-8 OLI data had a GSD of 30-meters. In addition, one set of Synthetic Aperture Radar (SAR) from Sentinel-1B (ESA 2018) for each year was collected from UAF (2019). The SAR data had a GSD of 15-meters. A digital elevation model (DEM) was collected from Alaska (2019). The DEM had a GSD of 30-meters. The final data set was canopy closure from the LandFire Project (USDA 2016). The canopy closure had a GSD of 30-meters.

The two sets of optical remotely sensed data (i.e. MODIS and LandSat8) were processed via Google Earth Engine® using methods outline in Chastain R, Houseman et al. (2019). MODIS and LandSat-8 OLI contained nine unique image bands. In order to get a comprehensive, cloud free, optical image, from both MODIS and LandSat, imagery needed to be collected over a 60-day time period, then mosaiced. This time period was the same for 2017 and 2018. The time period was Julian day 213 to 273 (i.e. 60-day time window).

The SAR data for both time periods were collected from Julian day 232 to 240 (i.e. eight-day time window). For 2017 ten SAR Single Look Complex (SLC) images were acquired and for 2018 eight SLC were needed. The SAR SLC data was processed using the Sentinel Application Platform (SNAP) (ESA 2019). In addition, the SAR SLC data was processed using methods outlined in SERVIR (2019). The SAR output data was two polarizations (VV and VH). Two additional SAR polarization products were generated: 1) a delta raster (VV – VH) and 2) a ratio product (VH/VV).

Three products were generated from the DEM: slope, aspect, and elevation. All the MODIS, LandSat, SAR, slope, aspect, elevation, and canopy closure were projected into the North American Datum of 1983 Alaska Albers, False Easting = 0.0 meters, False Northing = 0.0 meters, Central Meridian = -154.0°, 1st Standard Parallel = 55.0° N, 2nd Standard Parallel 65.0° N, Latitude of Origin = 50.0° N (ESRI 2019).

Using the positive and negative sample points for each year coupled with the optical imagery, SAR data, slope, aspect, elevation, and canopy closure data, a classification and regression tree (CART) (Ripley 2016) analysis was conducted using the statistical program R (R Development Core Team 2019). That is, using the sample points (positive and negative) as an independent categorical variable and the 26 data sets (i.e. nine LandSat bands, nine MODIS bands, four SAR data sets, slope, aspect, elevation, and canopy closure) as the depended continuous variables or covariates.

The steps used in the CART analysis are as follows. First, the continuous numerical values that were spatially coincident with the sample points were extracted using ArcGIS (ESRI 2019) from each of the covariates. Second, a text file containing positive and negative infestation values coupled with the spatial coincident 26 covariate numerical values were generated for each year. This output text file was the input to the CART program.

Classification and Regression Tree (CART) is a non-parametric machine learning statistical method for classifying both categorical and continuous data (De'ath and Fabricius 2000; Loh 2008; Tuffly 2017). Moreover, CART is not subject to spatial or temporal autocorrelation (Tuffly 2017). Therefore, it is a very useful method to classify remotely sensed imagery that is spatially and or temporally autocorrelated. Furthermore, CART uses a "Greedy Statistical Method" (GSM). A GSM removes covariates from the model which are not contributing to the accuracy (De'ath and Fabricius 2000). The output from CART is a decision tree. The decision tree identifies the important covariates coupled with break points to classify the data into the final product. In this case, the goal was to comprehensively classify the entire Cook Inlet ecoregion into areas that could suffer spruce mortality due to *D. rufipennis*.

Results

In 2017 the ADS data indicated that 11,410 hectares were infested with *D. rufipennis* (positive) out of 439,265 hectares surveyed (negative) (figure 4) for the Cook Inlet ecoregion. In 2018, the ADS data indicated that 40,026 hectares were infested (positive) with *D. rufipennis* out of 1,557,460 hectares surveyed (negative) (figure 5) for the Cook Inlet ecoregion.

The spruce basal area data set is static in nature. The spruce data set for the entire Cook Inlet ecoregions contains 4,596,614 square feet of basal area. The spruce basal area data illustrates that no spruce is found above 784 meters in elevation. In 2017 the ADS data only sample positive areas that contained 1 to 61 square feet of basal area per acre. Whereas the negative areas for 2017 contained areas from 1 to 117 square feet of basal area per acre. In 2018 the ADS data only sample positive areas that contained 1 to 70 square feet of basal area per acre. Whereas the negative areas for 2018 contained areas from 1 to 160 square feet of basal area per acre. A bar chart illustrating the cumulative basal area by elevation is found in figure 8.

The ADS data for 2017 sampled elevation areas ranging from 1 meter to 458 meters. In addition, the negative areas for 2017 encompassed regions from 1 meter to 458 meters. Whereas the positive areas ranged from 7 meters to 427 meters in elevation. The 2018 ADS data sampled elevations ranging from 1 meter to 784 meters. In 2018 the elevations for the negative regions ranged from 1 to 784 meters. Whereas the positive areas in 2018 ranged from 1 to 638 meters in elevation.

The CART analysis for 2017 illustrated that elevation, MODIS band1, MODIS band4, SAR-VH, MODIS band7, and MODIS band3 were important covariates for the identification of spruce mortality due to *D. rufipennis* (figure 9). In 2018 the CART analysis indicated that elevation, LandSat band3, SAR-VH, and MODIS band4 were important covariates in the identification of spruce mortality due to *D. rufipennis* (figure 10).

Reading the decision tree is simple and straight forward. Here is a brief narrative for reading one branch of figure 9. If a location is less than 43.5 meters in elevation and MODIS band1 is less than 5,865.5 and MODIS band4 is less than 2,565,000; then, these data are classified as potentially suffering spruce mortality due to *D. rufipennis*. It is worth noting here, in this narrative example, that the terminus data set is the SAR-VH (figure 9). Furthermore, the SAR-VH data produces both positive spruce mortality due to *D. rufipennis* regardless of the SAR values. This might be somewhat confusing to someone unfamiliar with CART. In summary, each one of the positive outcomes from the SAR-VH data have a different probability of spruce mortality. Once the classification logic (i.e. covariates and break points) are identified for each time period via the CART output, it is a straight forward process to implement the methodology in the programming language python (Rossum, Hammond et al. 2018) for the comprehensive classification of the entire ecoregion.

Once the covariates and break points were identified by the CART analysis. The data were classified using the aforementioned parameters via a custom python program. In addition, a mortality probability was also assigned to each positive component of the CART analysis.

It is worth noting that elevation is a static covariate for this study. Moreover, elevation was found to be an important parameter. Finally, the break points for elevation were the same in both 2017 and 2018 (i.e. 43.5 meters in elevation). The Cook Inlet contains 567,527 hectares (18.67% of the total ecoregion area) that are less than or equal to 43.5 meters in elevation.

At this point in the analysis there are two classified images for the Cook Inlet ecoregion. One image for 2017 and the other is for 2018. The probability of spruce mortality due to *D. rufipennis* for 2017 and 2018 is known and contained in figure 11 and figure 12, respectively. Illustrated, in figure 11 there are three probabilities for spruce mortality due to *D. rufipennis*. That is, the CART analysis indicated that there are three positive probabilities (55%, 83%, and 55%) spruce mortality due to *D. rufipennis*.

The objective of this study is to identify potential spruce stand mortality. The ADS data for 2017 indicated, at a conservative level, that all the positive sample points were in stands that had spruce mortality of 40%. Therefore, taking the three probabilities generated from CART for 2017 (figure 11) (i.e. 55%, 83%, and 55%) and multiplying by the 40% stand mortality; the final outcome would be the modeled probability of spruce mortality over the entire ecoregion by year. The probability of mortality of a spruce stand due to *D. rufipennis* infestation is 22% or 33.2%. For 2018 the CART analysis indicated that there is only one probability for spruce mortality which is 68%. Following the same probability calculation which was implemented for the 2017 data illustrates that spruce stand mortality in 2018 is 27.5%. The spruce stand mortality probability partitioned by area for 2017 and 2018 are shown in table 3 and table 4, respectively. The total area for the Cook Inlet is 3,038,642 hectares. For 2017 there is a 22% chance for spruce mortality due to *D. rufipennis* on 68,250.25 hectares and a 33.20% probability for spruce mortality due to *D. rufipennis* on 96,531.84 hectares (total is 164,782 hectares or 5.42% of the entire Cook Inlet ecoregion). For 2018 there is a 27.5% probability of tree mortality due to *D. rufipennis* on 212,908.14 hectares or 7.01% of the entire Cook Inlet ecoregion.

The next step was to calculate potential forest basal area loss for the Cook Inlet ecoregion for 2017 and 2018. The process for computing basal area loss involved using two data sets for each year. The first data set was the probability surface depicting spruce mortality by year and the second was a spruce basal area surface from the USFS (2019). Thus, multiplying the probability of mortality by the basal area produced a surface which showed the potential spruce basal area loss for 2017 and 2018 due to *D. rufipennis* infestation figure 13 and figure 14, respectively. Table 5 and table 6 summarizes the basal area losses for the Cook Inlet for 2017 and 2018, respectively.

To predict the potential tree mortality that could occur for 2019 a cumulative probability surface was created. That is, adding the probabilities for 2017 to 2018 to produce a surface for 2019 was implemented (figure 15). This produced five classes of probabilities ranging from a low of 22% to a high of 60.4% and a total area of 376,458.84 hectares or 12.39% of the total area of the Cook Inlet (table 7). In addition, for 2019 a basal area lost surface was generated using the same methods which generated the 2017 and 2018 basal area loss surfaces (figure 13). Finally, a table was created that shows the hectares loss by basal area for 2019 (table 8).

Accuracy Assessment

A common method for implementing accuracy assessment using remotely sensed data (i.e. MODIS, Landsat, SAR) is the confusion matrix (Congalton, Green et al. 1993) (Tuffly 1995). Therefore, a confusion matrix was generated for the Cook Inlet for 2017 and 2018 and the results are contained in table 9 and table 10, respectively. Table 9 indicates that the overall accuracy for 2017 is 73.78%. However, to break this down by each class (positive and negative) it is evident that the negative class is 90% accurate; whereas, the positive is 45% accurate. In addition, in 2018 (table 10) the overall accuracy is 77.05%. Nevertheless, the negative class for 2018 was 93.5% accurate and the positive class was 25.05% accurate. A flow chart, illustrating the data processing steps is in figure 16.

Discussion

The spatial data used in this analysis for this remote area of Alaska are somewhat scant in nature. Nevertheless, these data are the best available at this time. When conducting spatial and temporal modeling it is optimum to have field samples that encompass the spatial extent of the area of interest coupled with the full range of values contained in the important covariates.

Clearly, it is physically and financially infeasible to collect wall to wall comprehensive ADS data on an annual basis for the entire Cook Inlet. Therefore, the only reasonable solution is to sample sections of the ecoregion from year to year. Nevertheless, sampling sections of an ecoregions may produce spatial and temporal data gaps. Data gaps can produce erratic results when conducting spatial and temporal modeling over a large ecoregion, such as the Cook Inlet.

The CART analysis, as with any other statistical tests, is extremely sensitive to data gaps. In this study, CART cannot predict positive spruce mortality if there are not data to support a positive infestation. Hence, by default these areas, with data gaps, would subsequently be classified as regions of negative infestation provided that at least one square foot of basal area was present.

The CART analysis for both 2017 and 2018 indicated that 43.5 meters in elevation was an important parameter. However, in 2017 positive areas were modeled both above and below 43.5 meters in elevation. Whereas in 2018 CART illustrated that no positive infestations were modeled below 43.5

meters in elevation. It is unclear at this point in time, if this is an artifact of where the ADS data were sampled from 2017 to 2018 or is this a case highlighting the fact that *D. rufipennis* is indeed migrating to higher elevations due to warmer air temperatures.

The static spruce basal area data set was finalized by the USFS in 2012. Currently, the metadata from the USFS on these data are unavailable. However, it is safe to say the data used to generate the 2012 basal area for the Cook Inlet are at least fifteen-years old or older. Thus, changes in basal area, during this fifteen year or so time gap, are not reflected in this static spruce basal area data set. Hence this is clearly a data gap.

The entire Cook Inlet contains a total of 4,596,614 square feet of basal area. Below 43.5 meters in elevation there is 616,011 square feet of basal area. In addition, from 43.5 meters to 784 meters there is 3,980,603 square feet of basal area.

The cumulative basal area by elevation (figure 8) illustrates that the highest probability of finding any basal area of spruce over the landscape will be in locations that are less than 50 meters in elevation. Furthermore, regions that contain 1 to 5 square feet of basal area per acre cover the highest percentage of area for the entire ecoregion when compared to any other basal area class (table 2). This typifies the fact that stands of spruce trees with basal area between 1 to 5 square feet per acre that are located below 50 meters in elevation have the highest probability of being selected. Nevertheless, this analysis, illustrated in table 5 and table 6, highlights the fact that areas with 1 to 5 square feet of basal area have the highest probability of mortality due to *D. rufipennis* infestation.

The spruce forest type in the Cook Inlet is subject to a short growing season, harsh climates, and marginal soil conditions; in addition, perturbations such as wildfire, avalanches, and flooding are also prevalent. These environmental and edaphic factors are the most likely contributors to the low basal area values found in the ecoregion. Moreover, these environmental and edaphic factors are likely to be extreme stress components of the spruce stands. Thus, predisposing these low basal area stands to *D. rufipennis* infestation.

The most plausible explanations for the low positive percent accuracy are multipronged. First, is the fact that for both time periods a relatively small area was identified as being infested with *D. rufipennis* via the ADS data when compare to the total area of the Cook Inlet ecoregion. Second, the possible low sensitivity the multispectral data have with respect to the *D. rufipennis* infestation. Third, the moderate to low probability that the CART analysis calculated for spruce mortality due to *D. rufipennis*. Finally, it is clear that elevation is a key physical parameter in 2018. However, it is unclear if elevation is an important parameter for 2017. This shift in elevation from one year to another may also be a contributing factor to the low positive percent accuracy.

Viewing these results from a differing perspective may be appropriate. That is, in both 2017 and 2018 the accuracy of negative infestation was over 90%. Therefore, if the model can accurately identify areas that are not infested; hence, the that information would be useful as a management tool.

Optical multispectral data is strongly influenced by clouds and sun angles. Sun angles in the northern latitudes change rapidly from season to season. In addition, the Cook Inlet ecoregions is subject to frequent cloud cover during the spring and summer months. The construction of a comprehensive cloud-free optical multispectral data set for the entire ecoregion is a complex task. To accomplish this

task many cloud-free optical multispectral data scenes over a sixty-day time period had to be acquired and subsequently concatenated. The sixty-day time period began in early August and ended in late September for both 2017 and 2018. On August 1st the sun angle in Anchorage AK is 45.58° above the horizon. On September 30th the sun angle is 24.35°. Therefore, during this sixty-day time period the sun angle decrease 21.23° or 53.42%. This reduction in sun angle over time will produce large shadows. Shadows greatly alter the spectral reflectance of optical remotely sensed data. Classifying optical remotely sensed data, at the individual image band level, using mosaiced data from different time periods with large varying shadows, can produce erratic results.

SAR data is not influenced by cloud cover or shadows (SERVIR 2019); thus, multiple scenes, collected over a short time period, that comprehensively covering the entire ecoregion can be acquired and concatenated. However, processing SAR data in to analysis ready products is a complex task when compared to the processing of optical multispectral data.

SAR data is better at identifying forest structure; whereas, optical remotely sensed data is a better tool for identifying forest health conditions (Fernandez-Ordonez, Soria-Ruiz and Leblon 2009). This point is illustrated by the fact that SAR-VH data and the multispectral MODIS band4 were important covariates in this study for both time periods.

The Sentinel-1 cross-polarization VH backscatter data has been very useful in identifying forest structure (SERVIR 2019). This is due to the fact that the Sentinel-1 cross-polarization VH SAR backscatter data is well suited in the identification of horizontal and vertical forest structure elements (SERVIR 2019). These horizontal and vertical forest structure elements are ideal in the differentiation between live fully foliated stands and dead defoliated forest stands.

MODIS band4 contains a bandwidth that ranges from 545 to 565 nanometers. MODIS band4, is sensitive to reflected green visible light. Hence, low reflectance values in MODIS band4 indicate dead, dying, or missing photosynthetic vegetation in forest stands. Therefore, MODIS band4 does well in capturing the initial stage of forest stand mortality. That is, in the initial stage of mortality, foliage remains on the trees in the forest stand; however, the existing foliage is brown in color and has lost the green photosynthetic pigments.

Therefore, the SAR data does well at capturing forest stands that have been dead for one or more years and are defoliated. However, it cannot differentiate between green healthy fully foliated stands, and stands that are foliated; but, the needles are brown. Whereas optical remotely sensed data (i.e. MODIS band4) can identify stands than have been infested and are exhibiting brown needles.

Another important point is the fact that the infestation area of *D. rufipennis* in the Cook Inlet is growing annually. This is possibly due to the side effects of increased annual air temperatures. That is, *D. rufipennis* could be changing from bivoltine to univoltine. The metamorphosis from bivoltine to univoltine could increase the existing populations of *D. rufipennis* at an accelerated rate. Furthermore, *D. rufipennis* populations from southern latitudes could be colonizing areas in the northern latitudes. Finally, warmer temperatures can be stressing the spruce trees; thus, reducing their natural defenses to *D. rufipennis* infestations.

Conclusion

This two-year time study highlights the fact that *D. rufipennis* populations are growing in the Cook Inlet. The population growth can be a function of *D. rufipennis* changing from bivoltine to univoltine and or populations from southern latitudes colonizing areas in the northern latitudes. Furthermore, areas that contain low basal area of spruce (i.e. 1 to 5 square feet) are the most susceptible to infestation of *D. rufipennis* due to harsh environmental and edaphic conditions. Optical remotely sensed multispectral data is influenced by clouds and shadows. Therefore, optical remotely sensed data from different time periods, must be collected and concatenated. Optical remotely sensed data from different time periods can be problematic in assessing forest mortality in large ecoregions located in northern latitudes, such as the Cook Inlet. SAR data, is not influenced by clouds or shadows. Hence, SAR data can be collected and concatenated for a short time period for a large landscape. Therefore, SAR data is likely to be the optimal and cost effective remotely sensed data in the identification of forest disturbance due to *D. rufipennis* on an annual basis for the Cook Inlet ecoregion.

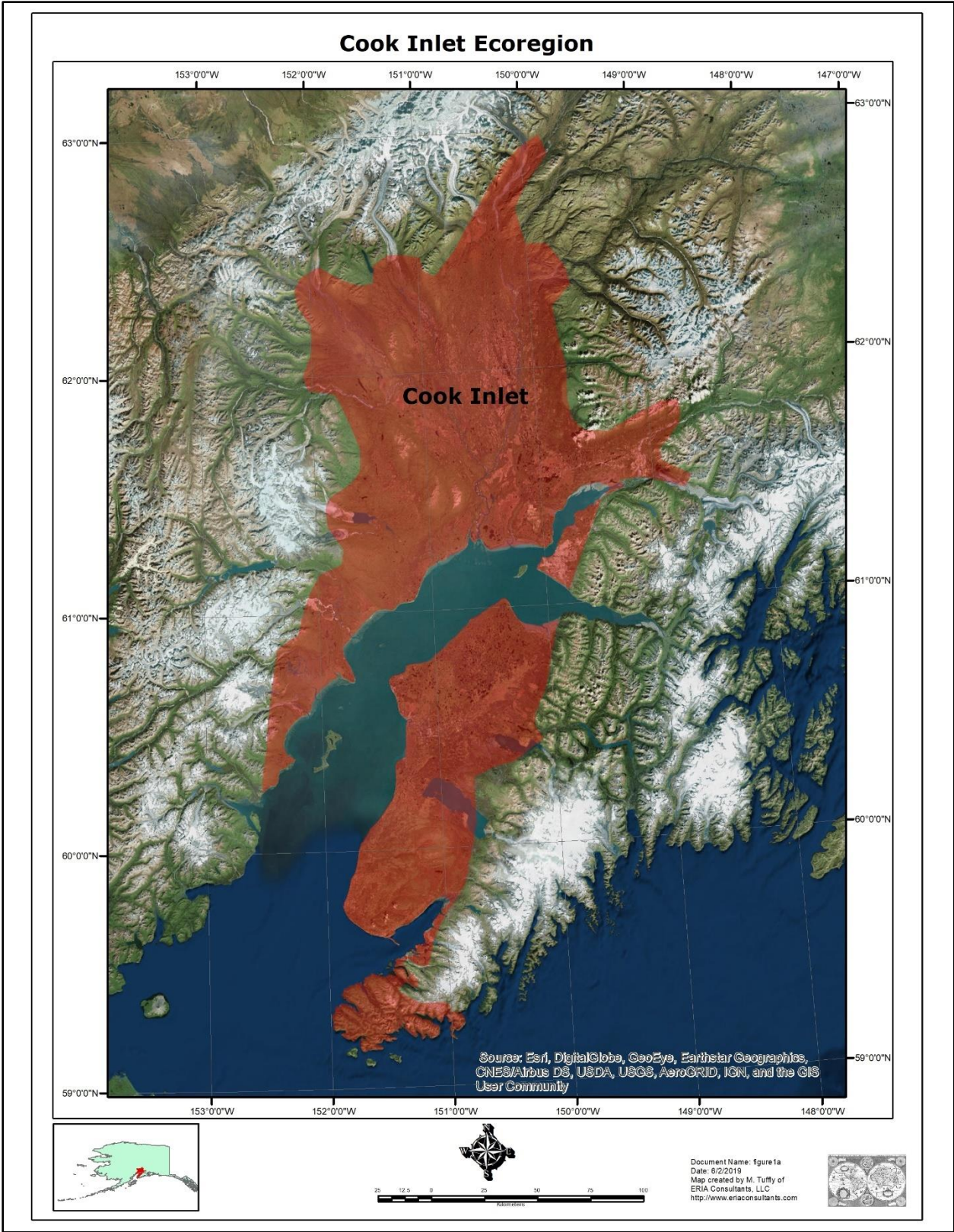


Figure 1.

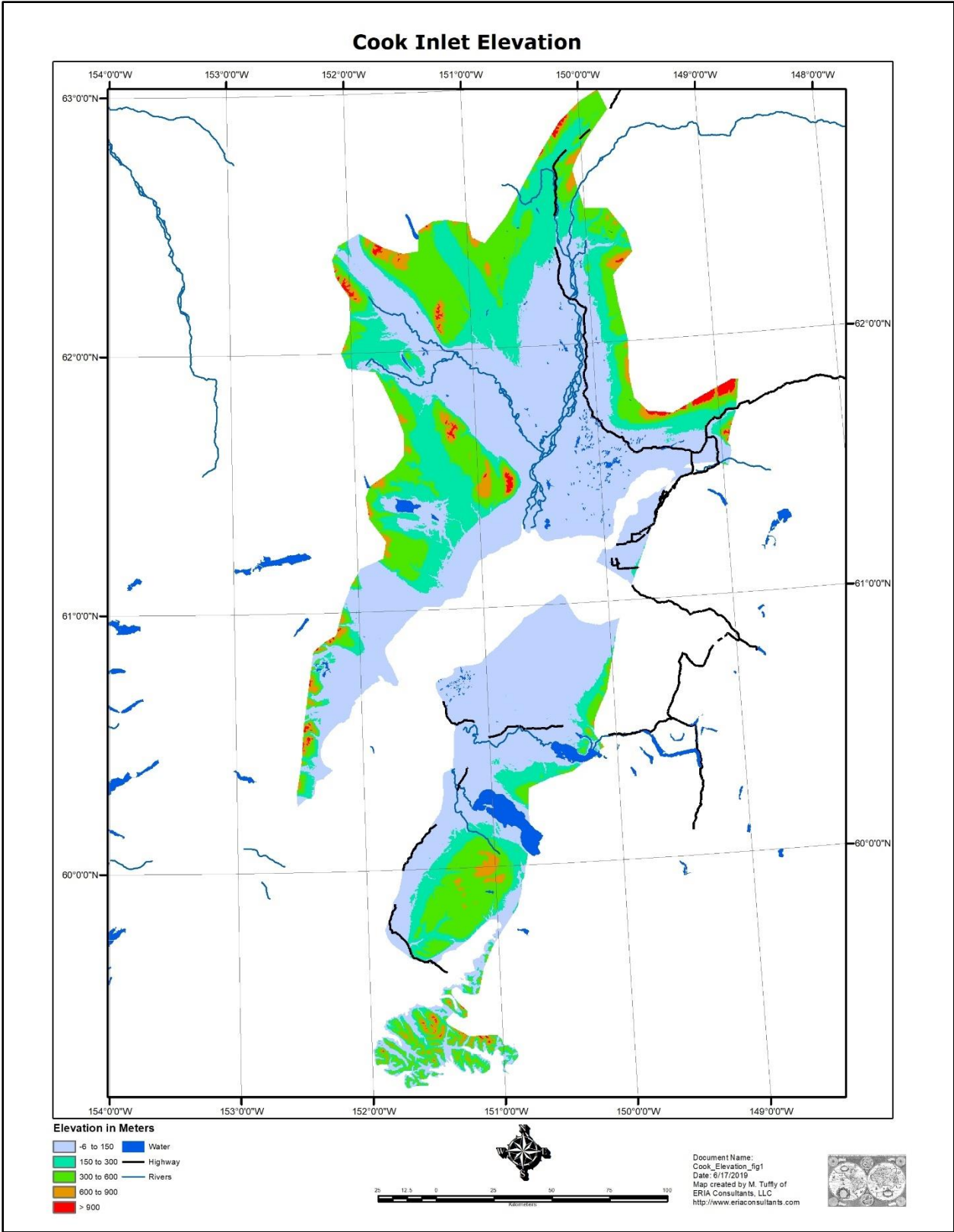


Figure 2.

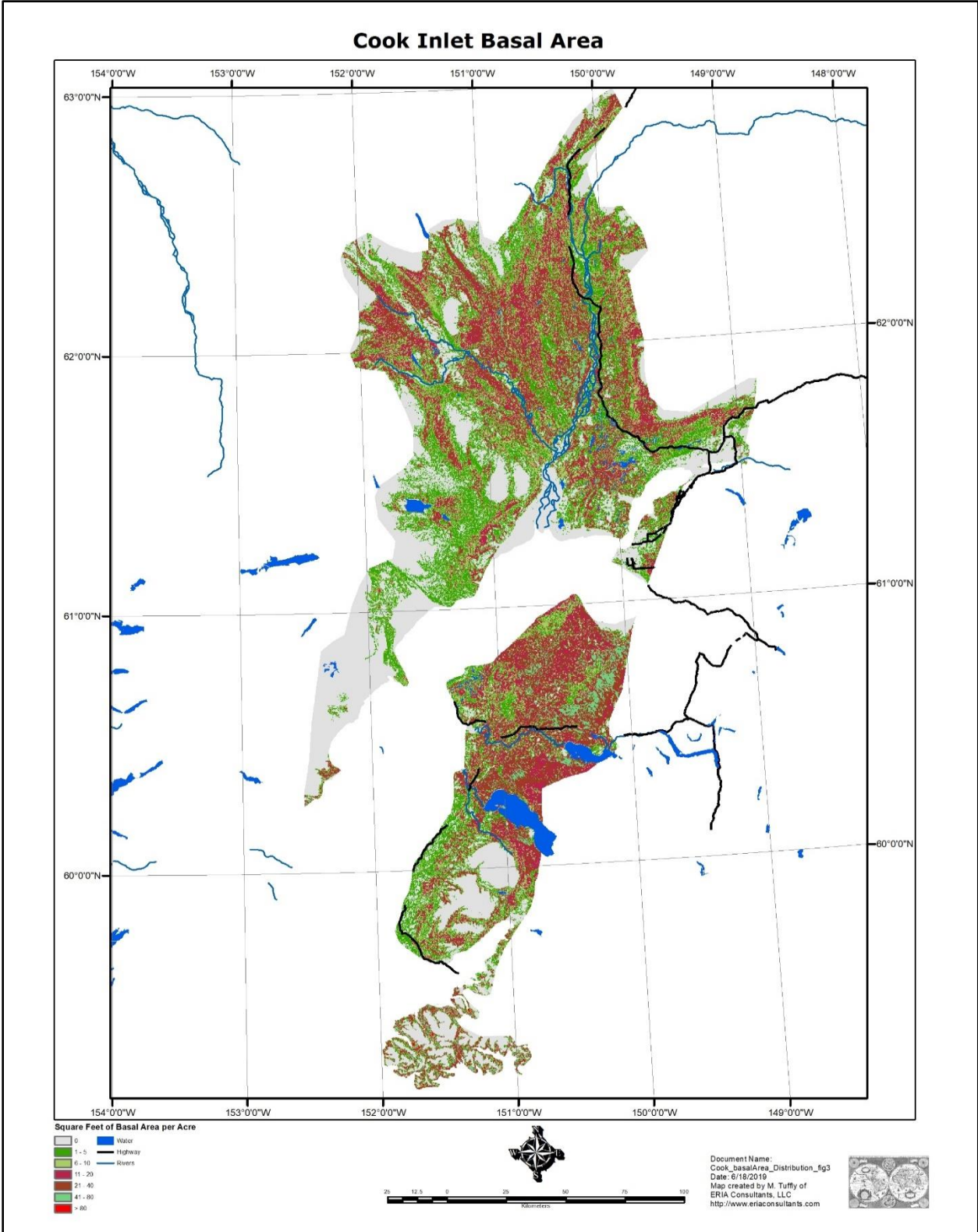


Figure 3.

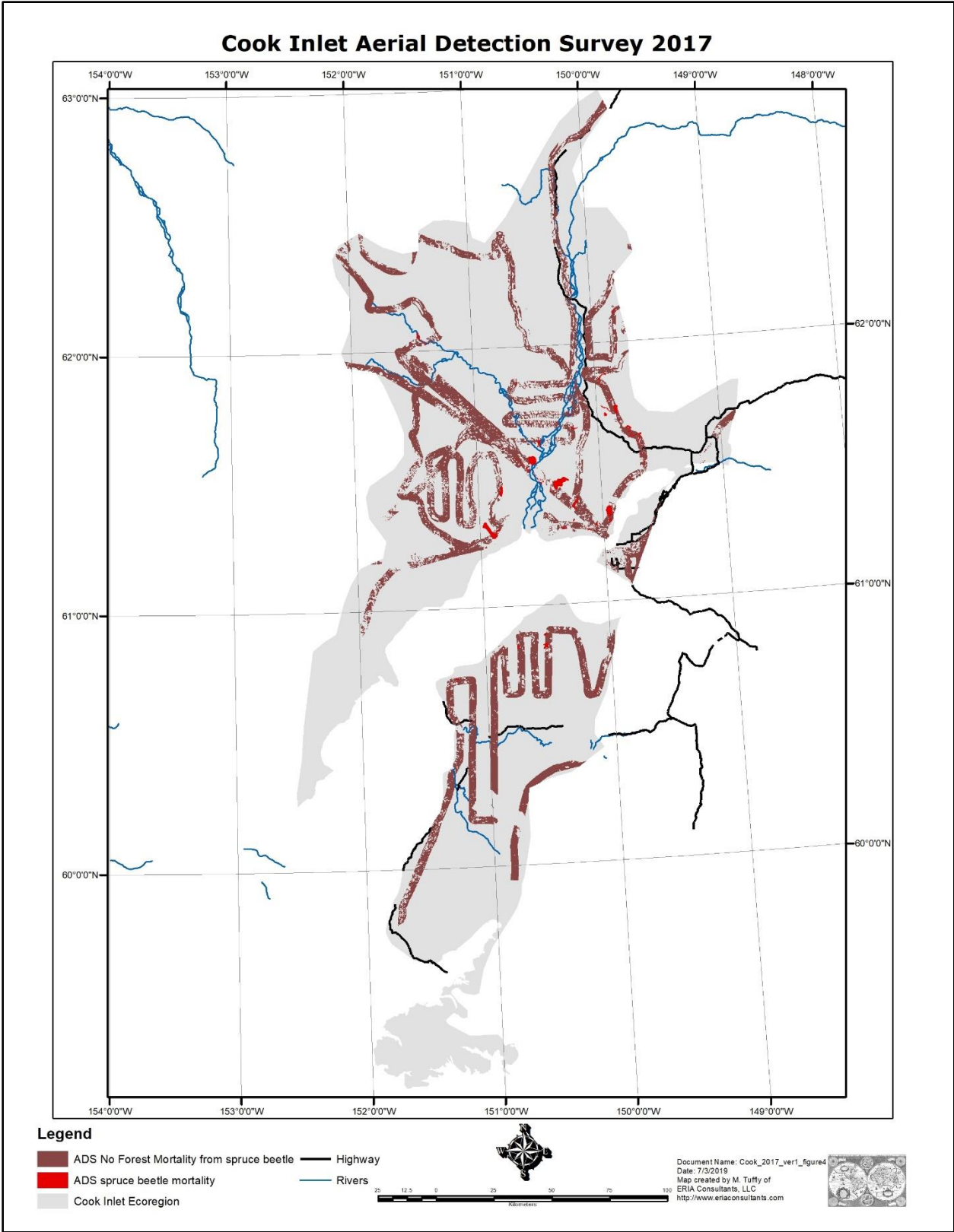


Figure 4.

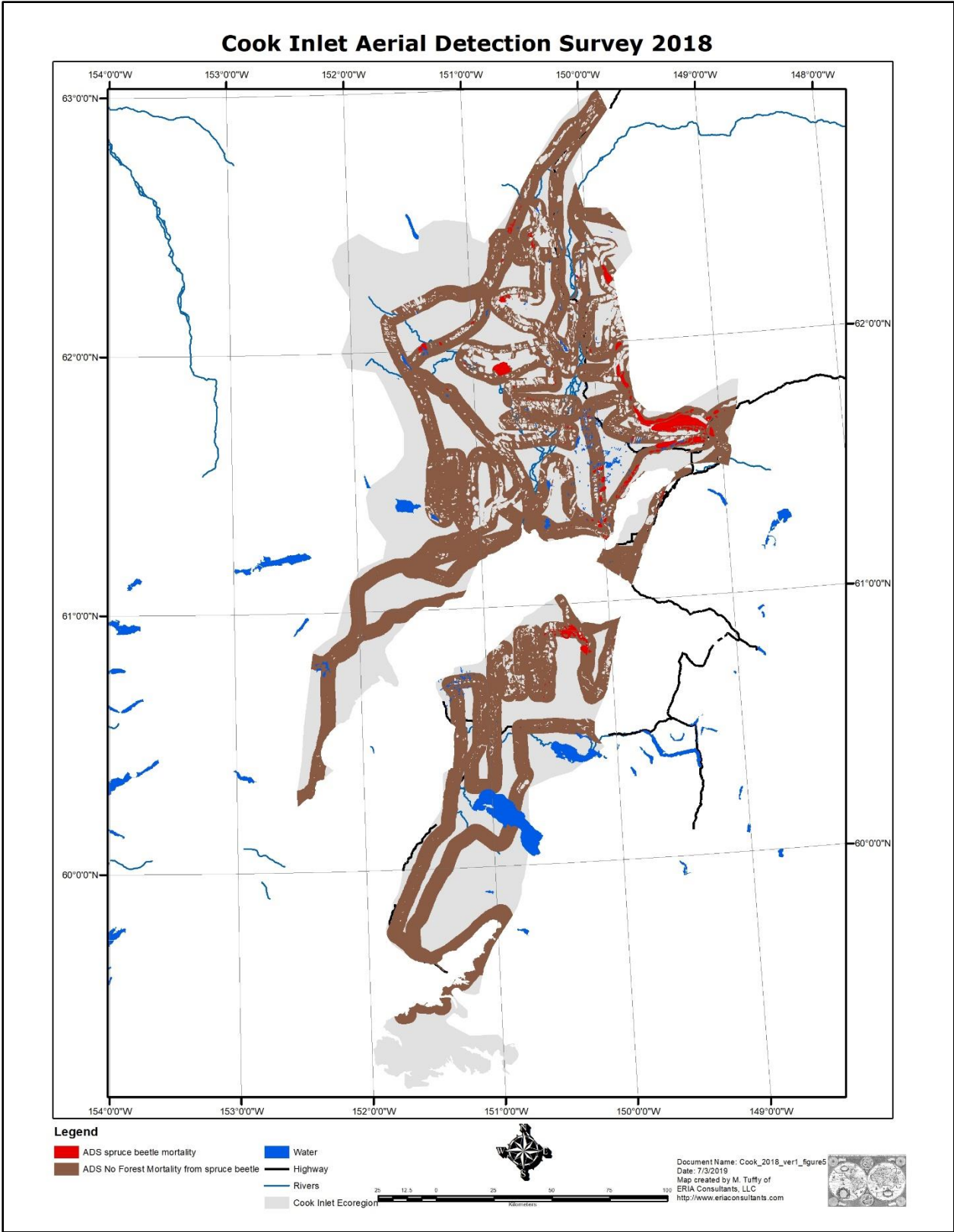


Figure 5.

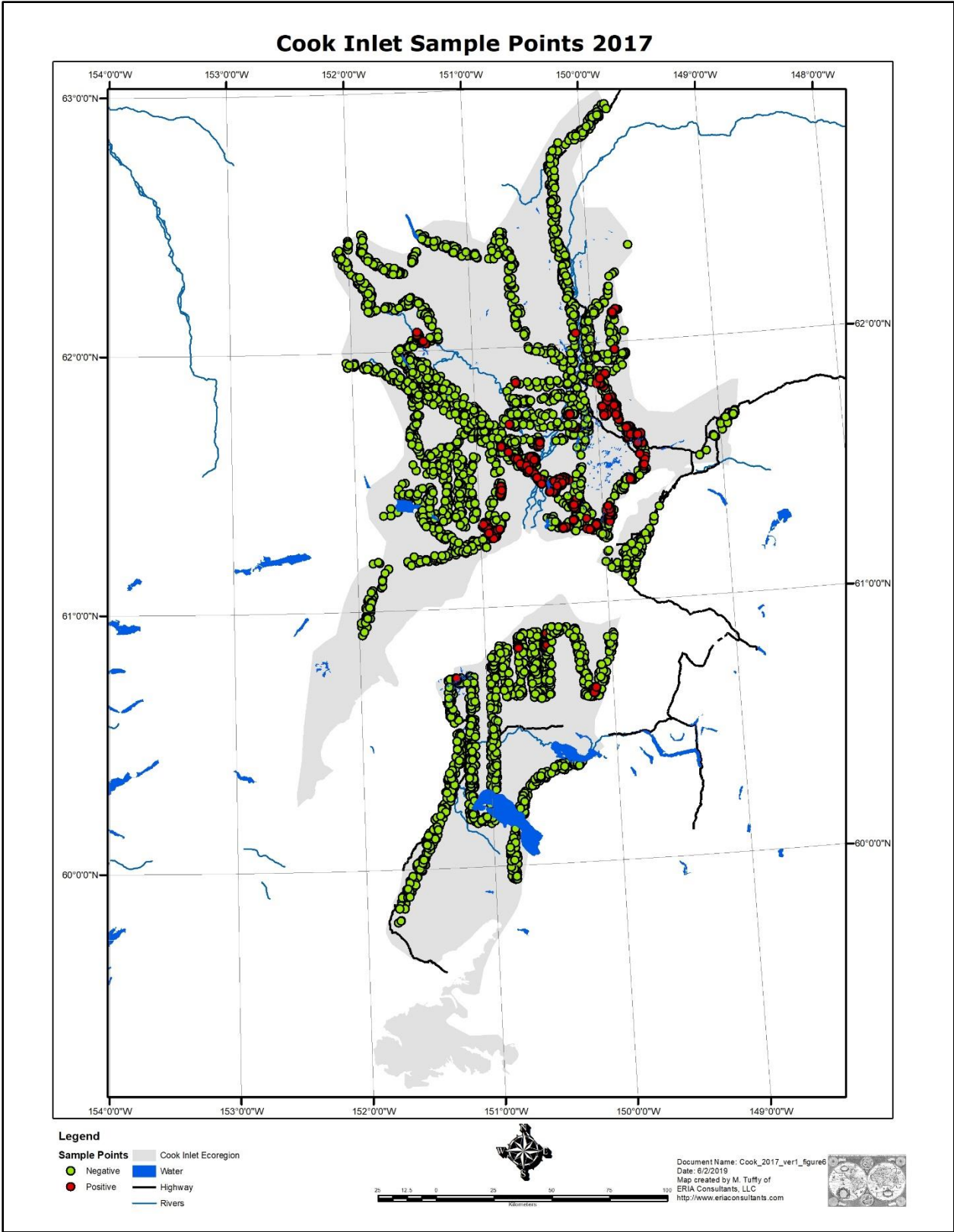


Figure 6.

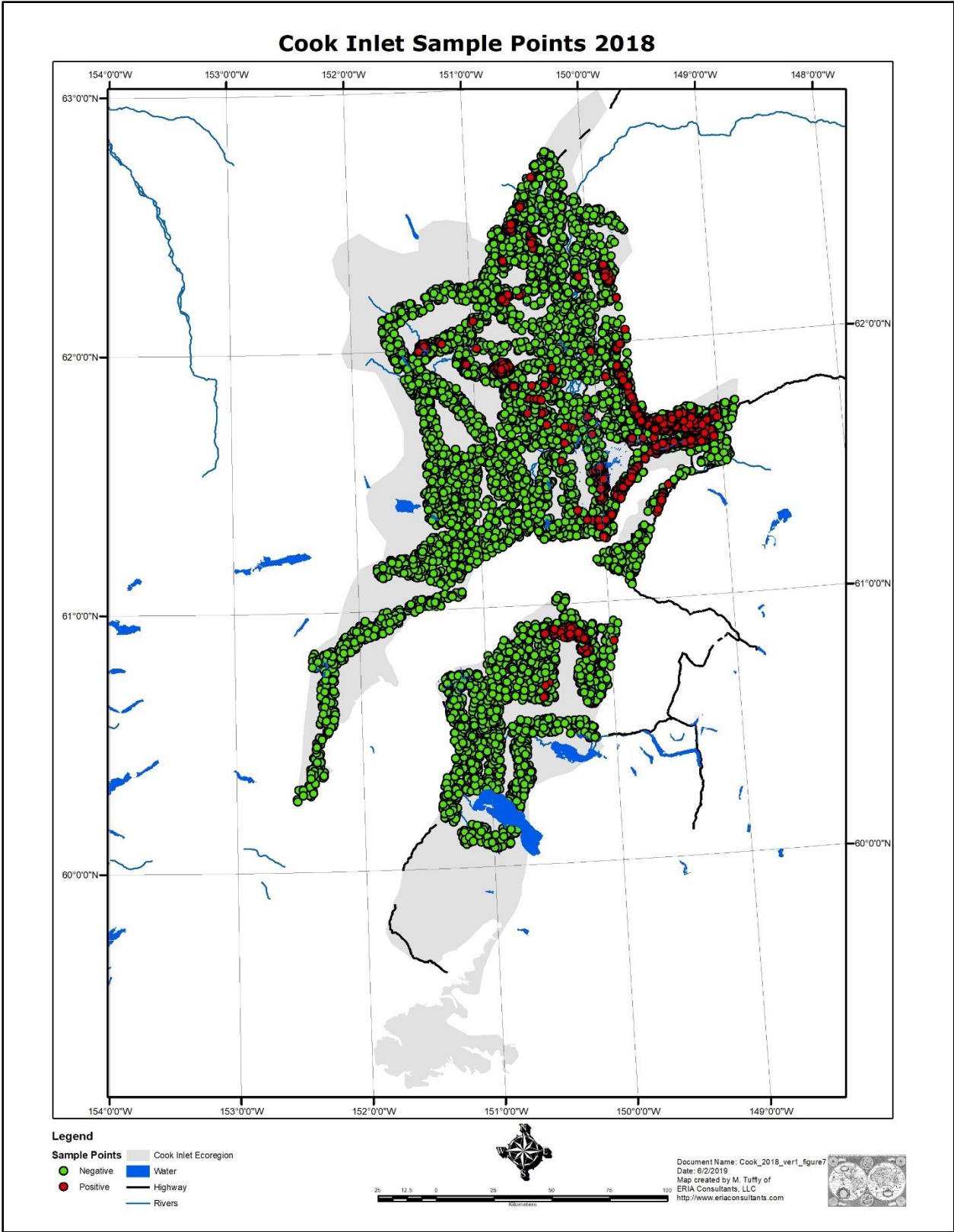


Figure 7.

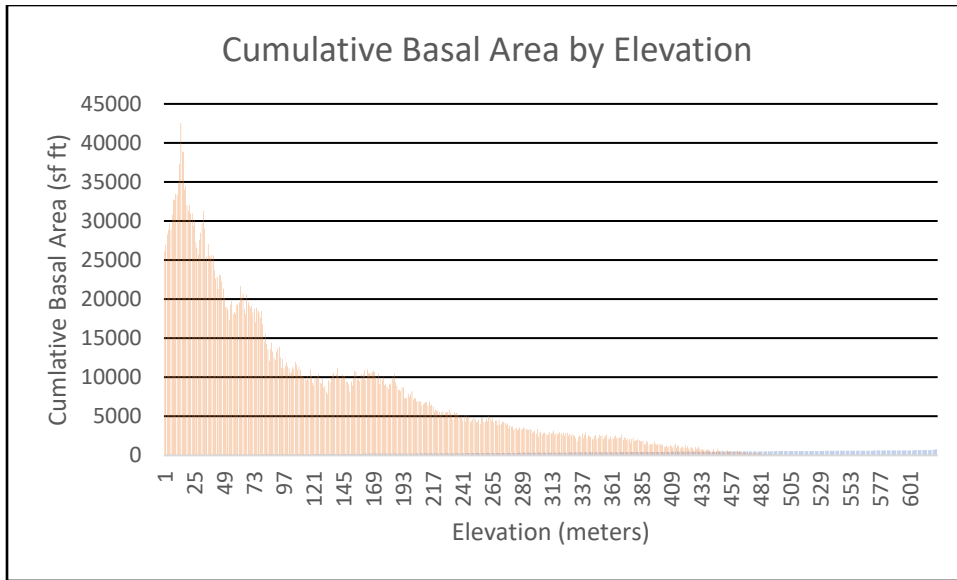


Figure 8.

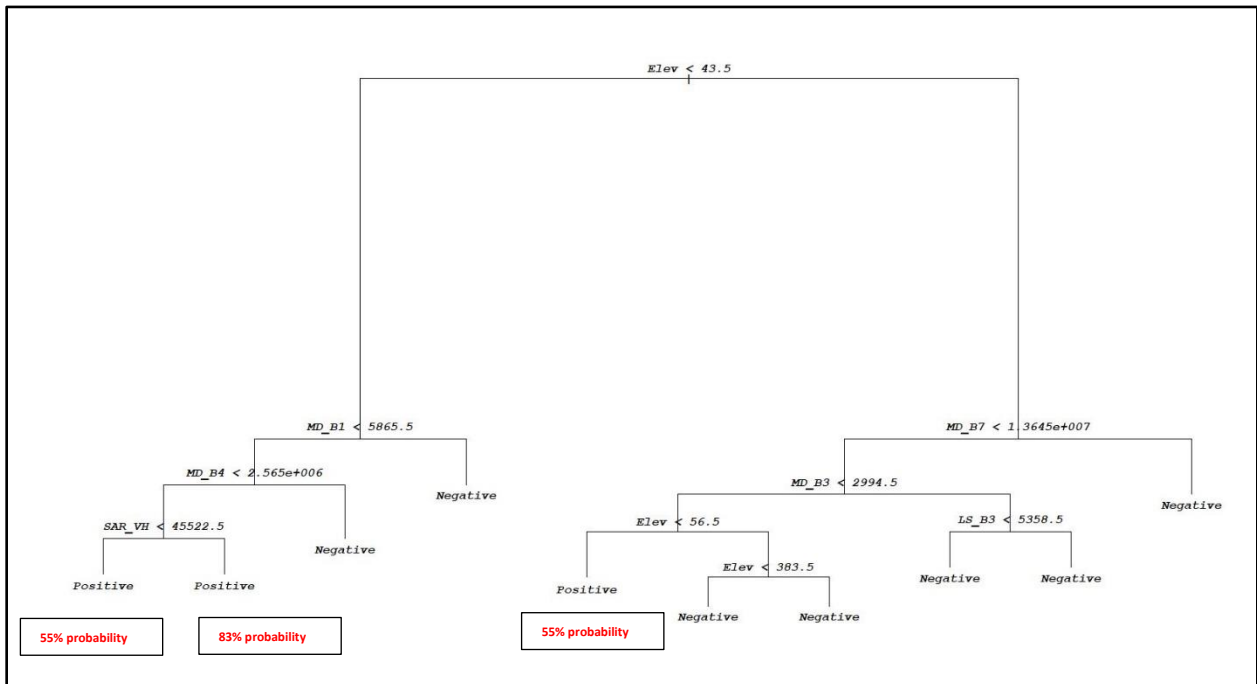


Figure 9. Classification and Regression Tree output for 2017.

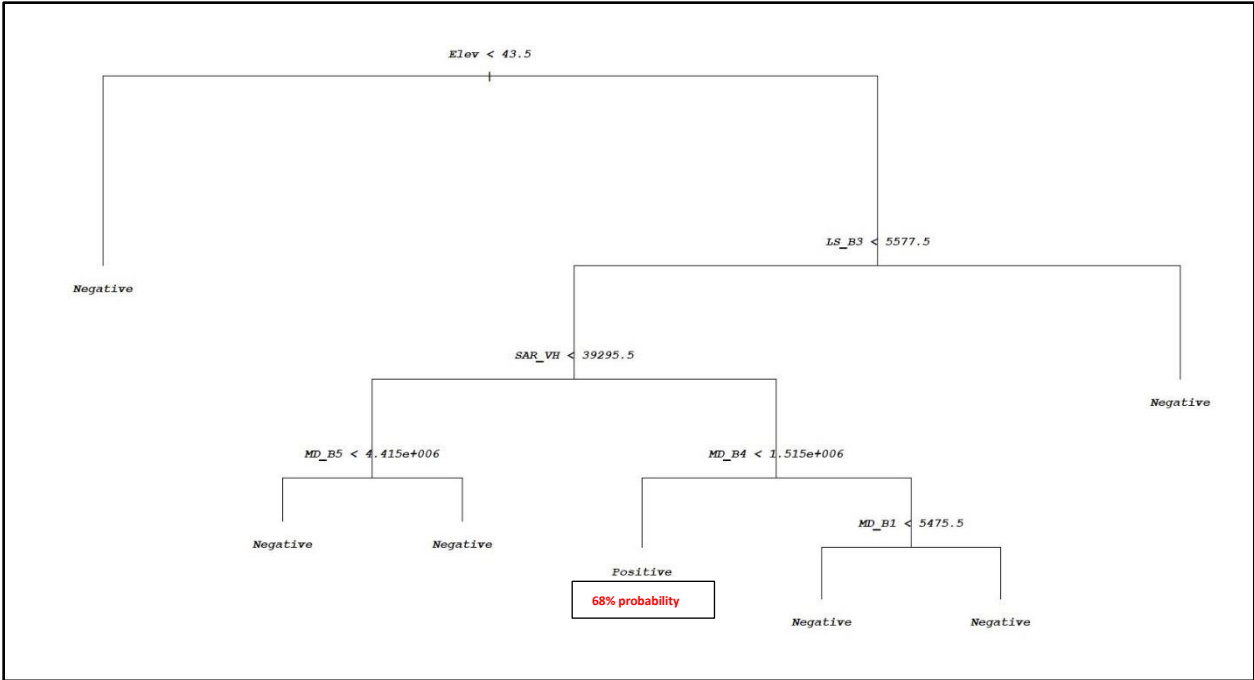


Figure 10. Classification and Regression Tree output for 2018.

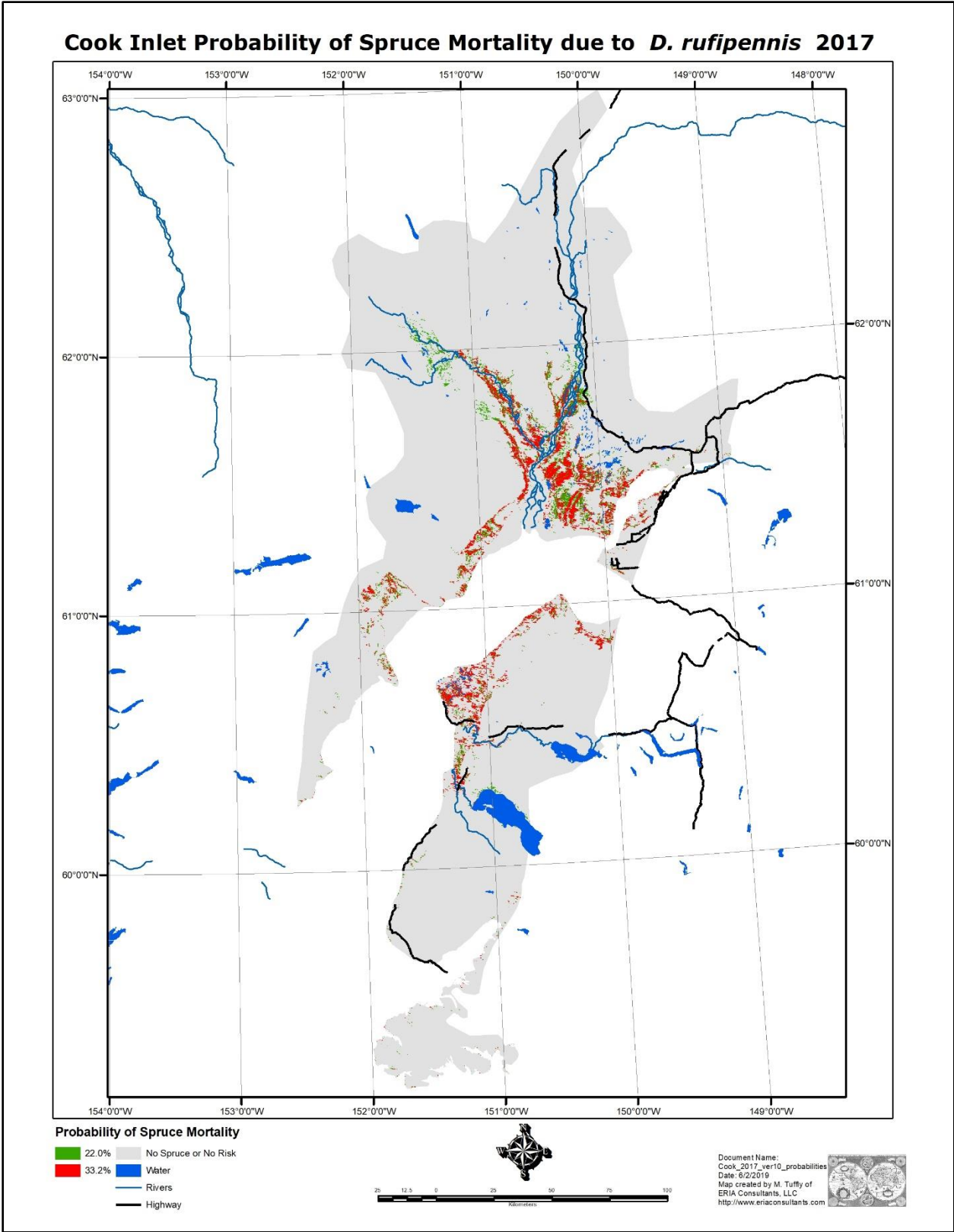


Figure 11.

Cook Inlet Probability of Spruce Mortality due to *D. rufipennis* 2018

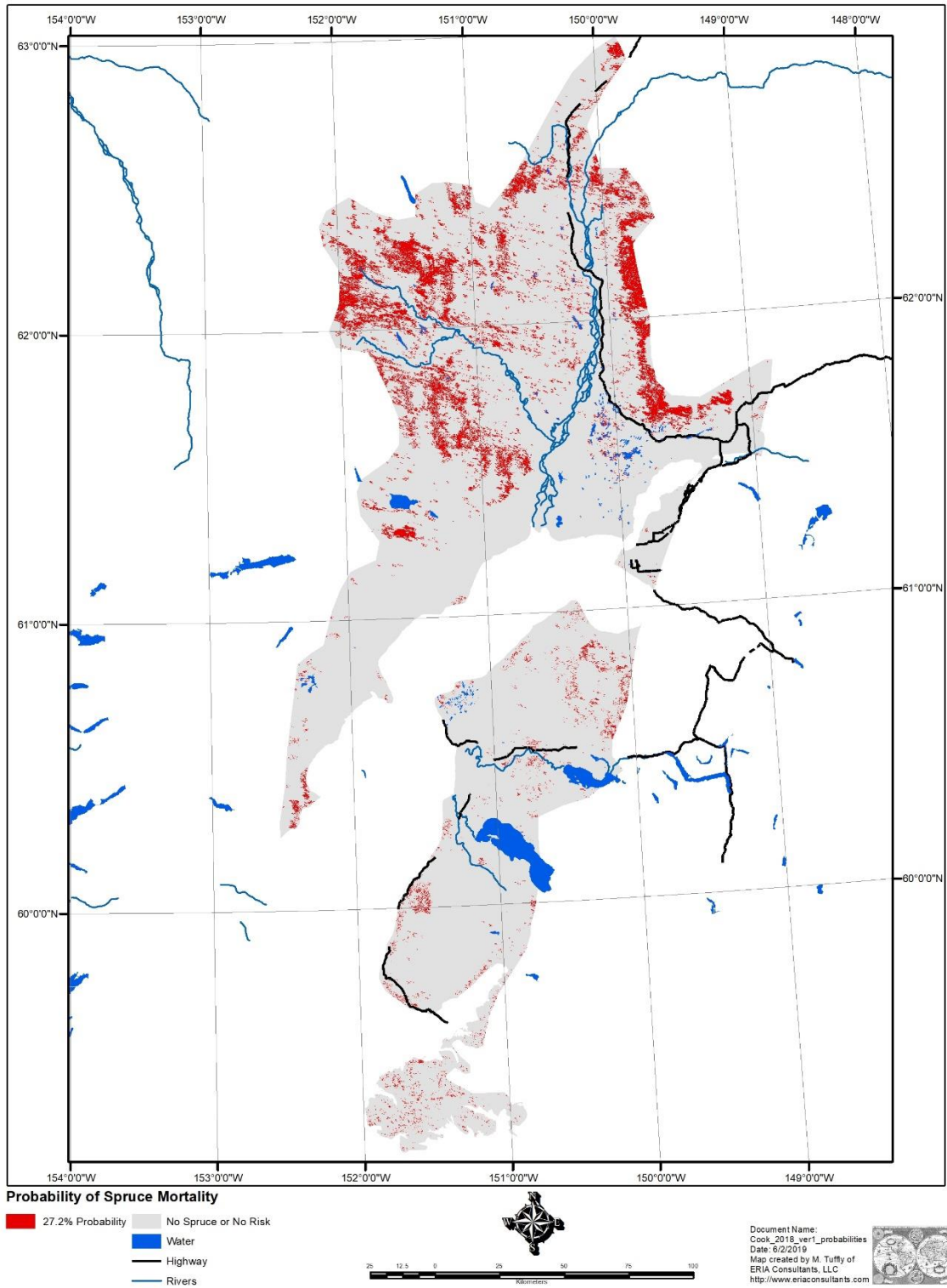


Figure 12.

Cook Inlet Total Potential Spruce Basal Area Loss due to *D. rufipennis* 2017

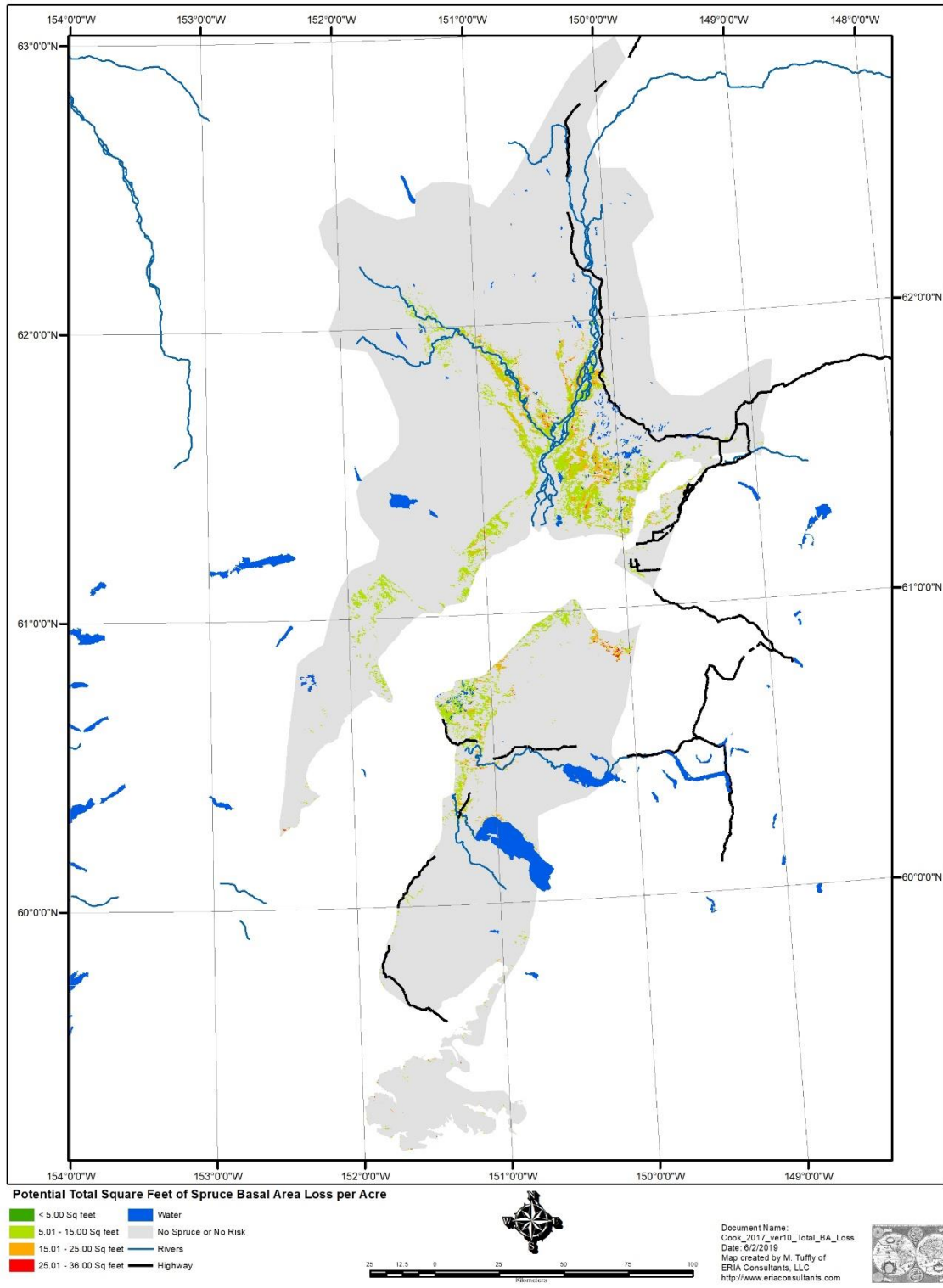


Figure 13.

Cook Inlet Total Potential Spruce Basal Area Loss due to *D. rufipennis* 2018

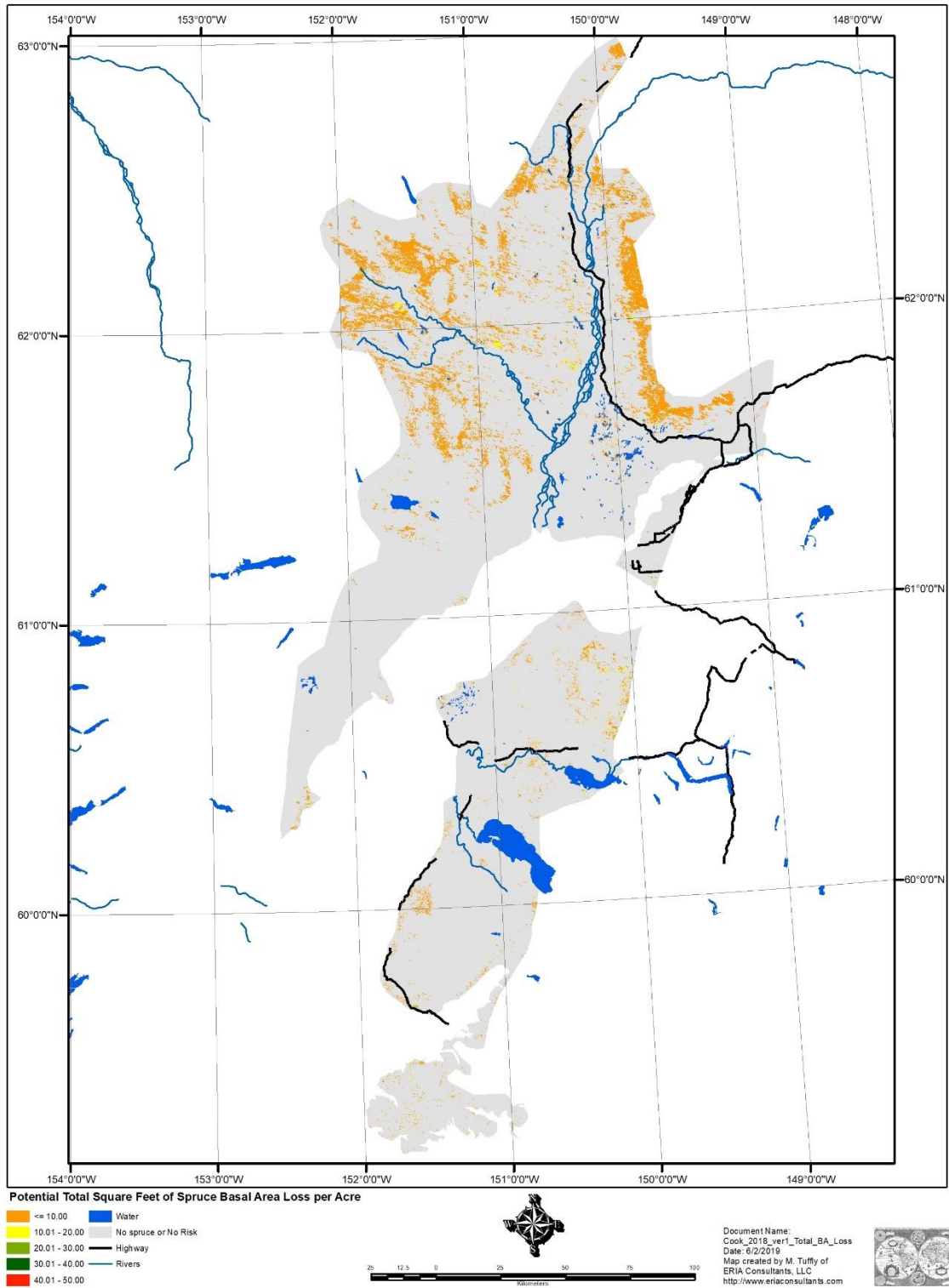


Figure 14.

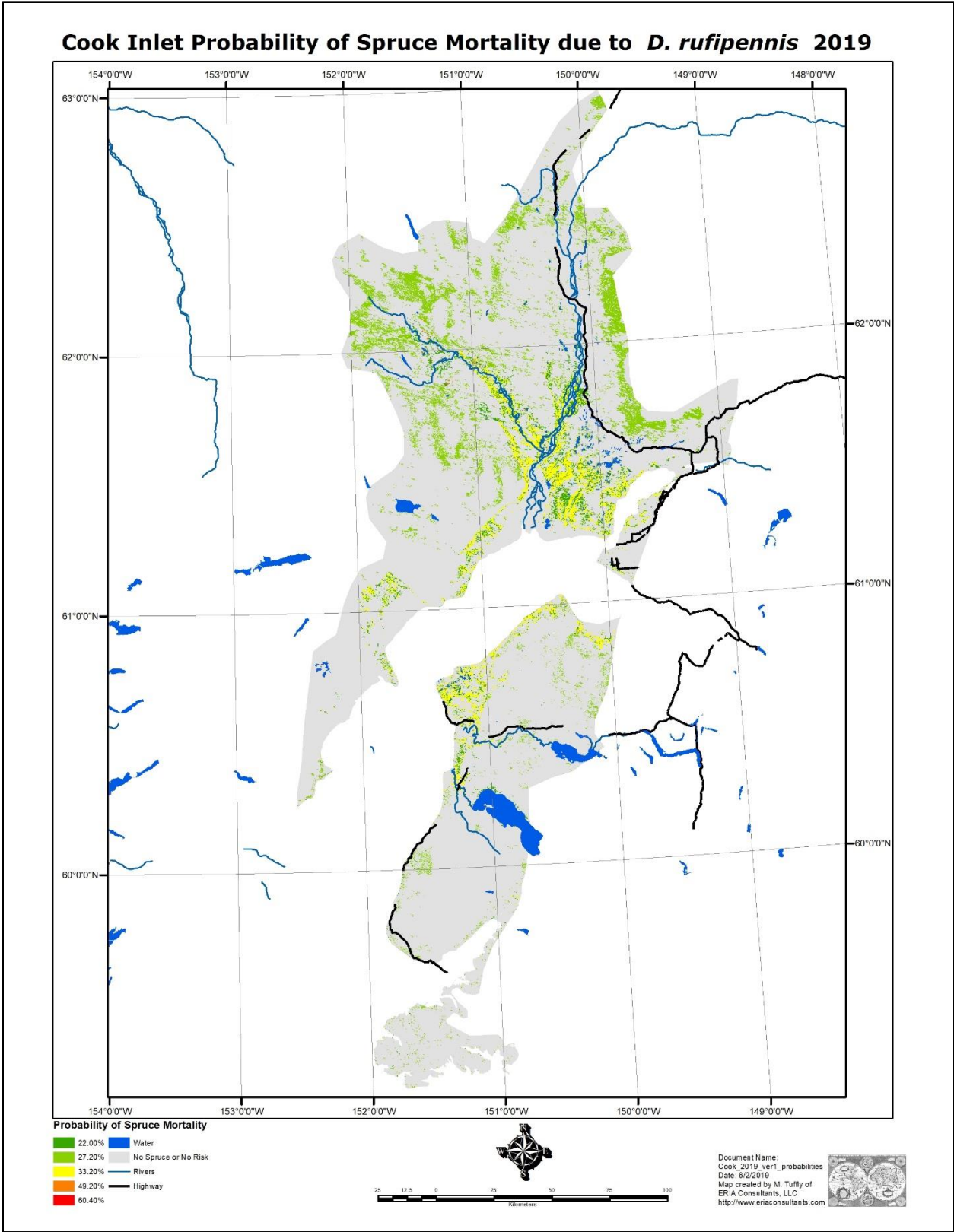
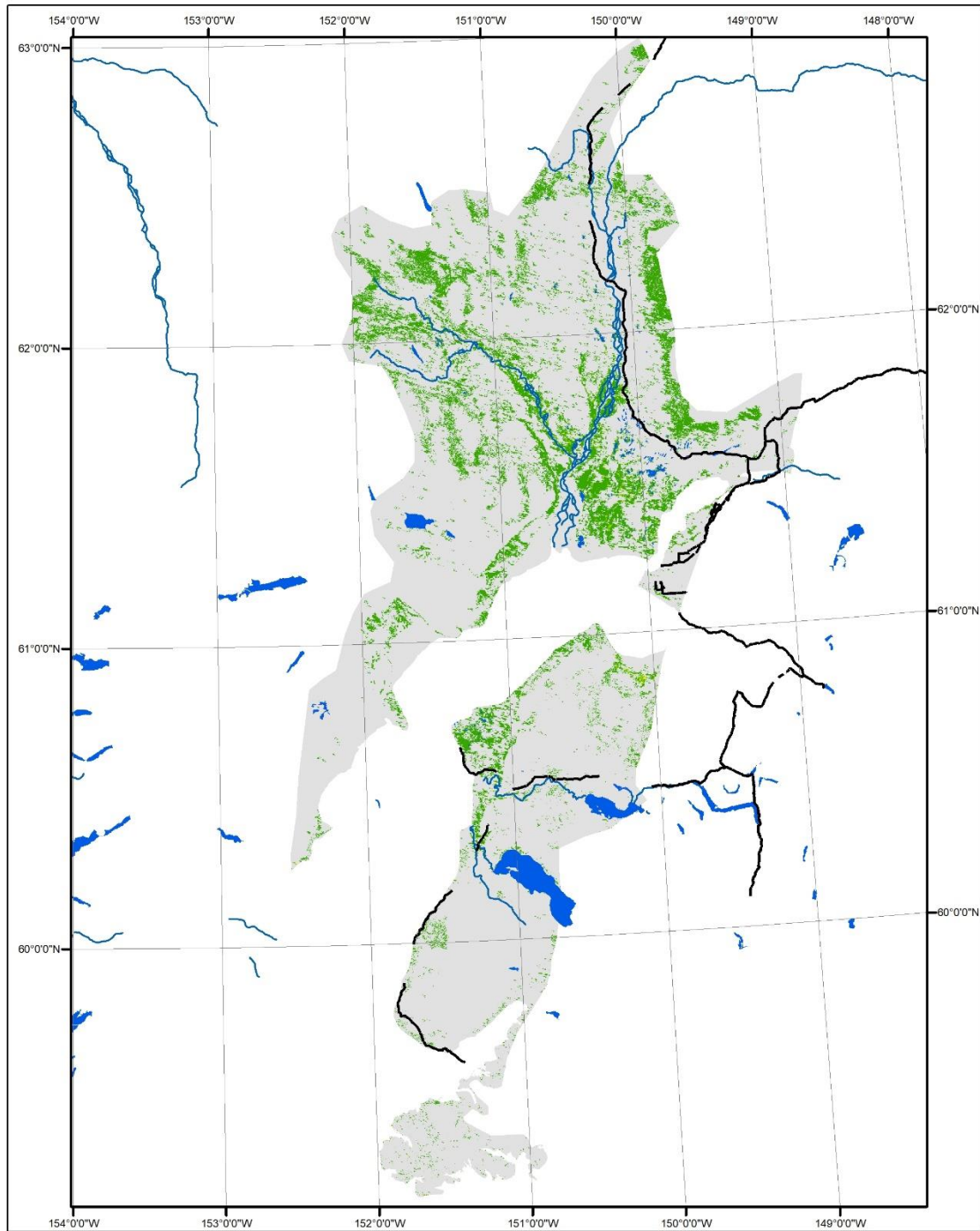
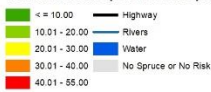


Figure 15.

Cook Inlet Total Potential Spruce Basal Area Loss due to *D. rufipennis* 2019



Potential Total Square Feet of Spruce Basal Area Loss per Acre



Document Name:
Cook_2019_ver1_Total_BA_Loss_figure14
Date: 6/2/2019
Map created by M. Tuffly of
ERIA Consultants, LLC
<http://www.eriaconsultants.com>



Figure 16.

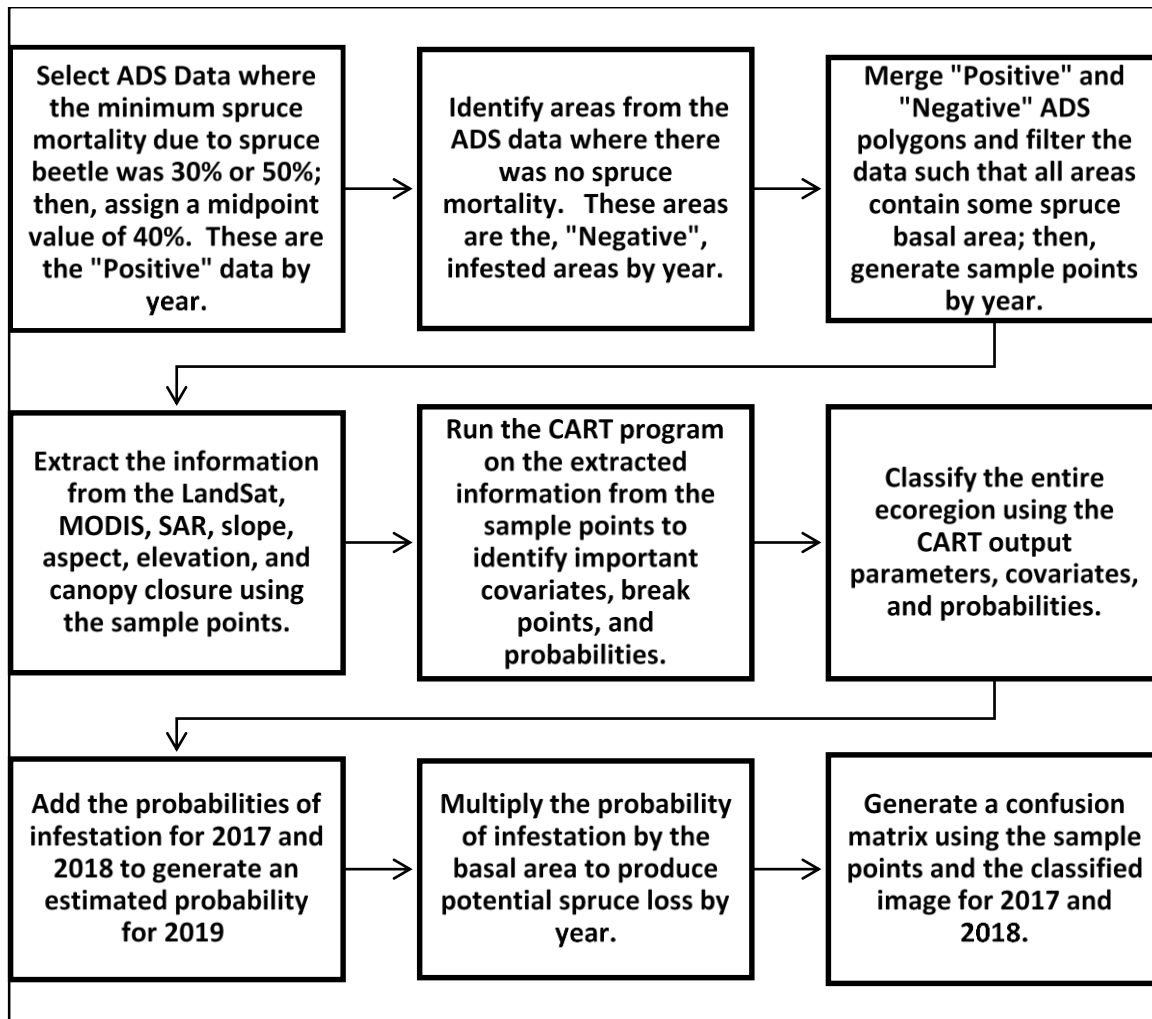


Figure 17. Data Processing Flow Chart.

Table 1. Elevation Ranges.

Elevation Range Values (meters)	Hectares	Percent Area
-6 to 150	1,692,611.98	55.70
151 to 300	658,954.98	21.69
300 to 600	551,824.98	18.16
600 to 900	107,694.48	3.54
> 900	27,555.58	0.91
Total	3,038,642.00	100.00

Table 2. Basal Area Ranges.

Square Feet Basal Area Per Acre	Hectares	Percent Area
0	911,428.65	29.99
1 to 5	682,255.65	22.45
6 to 10	491,219.65	16.17
11 to 20	554,544.65	18.25
21 to 40	300,240.65	9.88
41 to 80	91,210.45	3.00
> 80	7,742.25	0.25
Total	3,038,641.95	100.00

Table 3. Probability of spruce mortality due to *D. rufipennis* in the Cook Inlet 2017.

Probability of Spruce Mortality	Hectares	Percent of Ecoregion
22.00%	68,250.25	2.25
33.20%	96,531.84	3.18
Total	164,782.09	5.42

Table 4. Probability of spruce mortality due to *D. rufipennis* in the Cook Inlet 2018.

Probability of Spruce Mortality	Hectares	Percent of Ecoregion
27.50%	212,908.14	7.01
Total	212,908.14	7.01

Table 5. Potential spruce basal area loss per acre in the Cook Inlet due to *D. rufipennis* 2017.

Square Feet Basal Area Loss per Acre	Hectares	Percent of Ecoregion
< 5	129,588.48	4.26
5.01 - 15.00	33,413.76	1.10
15.01 - 25.00	1,670.40	0.05
25.01 - 36.00	109.44	0.00
Total	164,782.08	5.42

Table 6. Potential spruce basal area loss per acre in the Cook Inlet due to *D. rufipennis* 2018.

Square Feet Basal Area Loss per Acre	Hectares	Percent of Ecoregion
<= 10.00	204,500.79	6.73
10.01 - 20.00	8,140.86	0.27
20.01 - 30.00	216.54	0.01
30.01 - 40.00	42.12	0.00
40.01 - 50.00	7.83	0.00
Total	212,908.14	7.01

Table 7. Probability of spruce mortality due to *D. rufipennis* in the Cook Inlet 2019.

Probability of Spruce Mortality	Hectares	Percent of Ecoregion
22.00%	67,300.83	2.21
27.20%	211,676.76	6.97
33.20%	96,249.87	3.17
49.20%	949.41	0.03
60.40%	281.97	0.01
Total	376,458.84	12.39

Table 8. Potential spruce basal area loss per acre in the Cook Inlet due to *D. rufipennis* 2019.

Square Feet Basal Area Loss per Acre	Hectares	Percent of Ecoregion
<= 10.00	367,285.86	12.09
10.01 - 20.00	8,858.43	0.29
20.01 - 30.00	268.92	0.01
30.01 - 40.00	42.93	0.00
40.01 - 55.00	2.70	0.00
Total	376,458.84	12.39

Table 9. Confusion Matrix 2017.

		Field Data					
		Negative	Positive	Total	Omission (%)	Commission (%)	Accuracy (%)
Modeled	Negative	3152	348	3500	25.77	9.94	90.06
	Positive	1094	906	2000	27.75	54.70	45.30
	Total	4246	1254	5500			73.78

Table 10. Confusion Matrix 2018.

		Field Data					
		Negative	Positive	Total	Omission (%)	Commission (%)	Accuracy (%)
Modeled	Negative	5912	411	6323	20.23	6.50	93.50
	Positive	1499	501	2000	45.07	74.95	25.05
	Total	7411	912	8323			77.05

References

- Alaska (2019). "AK State Geo_Spatial Data Clearinghouse." Retrieved April 11th, 2019, from <http://www.asgdc.state.ak.us/>.
- Chastain R, I. Houseman, J. Goldstein, M. Finco and K. Tenneson (2019). "Empirical cross sensor comparison of Sentinel-2A and 2B MSI, Landsat-8 OLI, and Landsat-7 ETM+ top of atmosphere spectral characteristics over the conterminous United States " Remote Sensing of Environment **221**: 274-285.
- Congalton, R., K. Green and J. Tepley (1993). "Mapping old growth forest and park lands in the Pacific Northwest from remotely sensed data." Photogrammetric Engineering & Remote Sensing **59**(4): 529 - 535.
- De'ath, G. and K. E. Fabricius (2000). "Classification and Regression Trees: A powerful Yet Simple Technique for Ecological Data Analysis." Ecology **81**(11): 3178 - 3192.
- EPA (2013). "Level III Ecoregions of the Continental United States." Retrieved May 27th, 2019, from <https://www.epa.gov/eco-research/ecoregions>.
- ESA (2018). "Sentinal-1." Retrieved 1/13/2018, 2018, from <https://earth.esa.int/web/sentinel/missions/sentinel-1>.
- ESA (2019). "Sentinel Application Platform." SNAP 6.0.6. from <https://step.esa.int/main/toolboxes/snap/>.
- ESRI (2019). "ArcGIS." 10.7. from <http://www.esri.com>.
- Fairweather, M. L., J. McMillin, T. Rogers, D. Conklin and B. Fitzgibbon (2006). Field Guide to Insects and Diseases of Arizona and New Mexico Forests. Albuquerque, New Mexico, USFS.
- Fernandez-Ordonez, Y., J. Soria-Ruiz and B. Leblon (2009). Forest Inventory using Optical and Radar Remote Sensing. Rijeka, Croatia, Intech.
- Forrest, J. R. (2016). "Complex responses of insect phenology to climate change." Current Opinion in Insect Science **17**: 49-54.
- Hagle, S. K., K. E. Gibson and S. Tunnock (2003). Field Guide to Diseases and Insect Pest of Northern and Central Rocky Mountain Conifers. Washington DC, USA, United State Department of Agriculture, Forest Service.

- Loh, W. Y. (2008). Classification and Regression Tree Methods. Encyclopedia of Statistics in Quality and Reliability. K. Ruggeri, and Faltin. Madison, WI, Wiley: 315 - 323.
- Moreira, A., P. Prats-Iraola, M. Younis, G. Krieger, I. Hajnsek and K. P. Papatjanassiou (2013). "A tutorial on Synthetic Aperture Radar." IEEE Geosciences and Remote Sensing Magazine: 6 - 43.
- NASA (2013). "LandSat8-OLI." Retrieved 12/20/2016, from <http://landsat.gsfc.nasa.gov/landsat-8/>.
- NASA (2019). "TERRA." Retrieved May 27th, 2019, from <https://modis.gsfc.nasa.gov/>.
- R Development Core Team (2019). "*R: A language and environment for statistical computing*." R Foundation for Statistical Computing 3.520.
- Ripley, B. (2016). "Classification and Regression Trees." 1.0-35. Brian Ripley, from <https://cran.r-project.org/web/packages/tree/tree.pdf>.
- Rossum, G. v., M. Hammond, J. Hylton, T. Peters and M. Zadka (2018). "Python." Python ver 2.7.15.
- SERVIR (2019). The SAR Handbook Comprehensive Methodologies for Forest Monitoring and Biomass Estimations. Huntsville, Alabama, NASA.
- Sherriff, R. L., E. E. Berg and A. E. Miller (2011). "Climate variability and spruce beetle (*Dendroctonus rufipennis*) outbreaks in south-central and southwest Alaska." Ecology **92**(7): 1459-1470.
- Tuffly, M. (1995). Predicting Vegetation Type and Fire Hazard in the Smith River National Recreation Area Using a Geographic Information System. College of Natural Resources. Arcata, California, Humboldt State University. **Masters**.
- Tuffly, M. (2017). "Creating a Burn Severity Map Using Classification and Regression Tree (CART)." Retrieved 1/4/2018, 2018, from <http://www.eriaconsultants.com/documents/dNBR%20Process.pdf>.
- Tuffly, M. F. (2012). Modeling the Spatial and Temporal Dynamics of the Amber-Marked Birch Leaf Miner Infestation in Anchorage, Alaska. Department of Forest Rangeland Stewardship. Fort Collins, Colorado, Colorado State University, . **Ph.D.**: 74.
- UAF (2019). "Alaska Satellite Facility." Retrieved May 27th, 2019, from <https://vertex.daac.asf.alaska.edu/>.
- USDA (2016). "LandFire." Retrieved 5/3/2016, 2016, from www.landfire.gov.

USFS (2019). "Aerial Detection Surveys (ADS)." Retrieved May 27th, 2019, from https://www.fs.fed.us/foresthealth/technology/ads_standards.shtml.

USFS (2019, 2012). "GIS Data for the 2012 National Insect and Disease Map Report." Retrieved May 28th, 2019, from <https://www.fs.fed.us/foresthealth/applied-sciences/mapping-reporting/gis-spatial-analysis/national-risk-maps.shtml>.

van Driesche, R. G., J. Laforest, C. Barger, R. Reardon and M. Herlihy (2019). "Forest Pest Insects in North America: a Photographic Guide." Retrieved May 29th, 2019, from <https://www.forestpests.org/vd/30.html>.

Williams, D. W. and A. M. Liebhold (2002). "Climate change and the outbreak ranges of two North American bark beetles." Agricultural and Forest Entomology **4**: 87-99.